A nucleolar targeting signal in PML-I addresses PML to nucleolar caps in stressed or senescent cells

Wilfried Condemine*, Yuki Takahashi*, Morgane Le Bras and Hugues de Thé‡

CNRS/Université de Paris 7 UMR7151, Equipe labellisée par la Ligue Contre le Cancer, Hôpital St. Louis, 1 Av. C. Vellefaux 75475, Paris Cedex 10, France

*These authors contributed equally to this work
‡Author for correspondence (e-mail: dethe@univ-paris-diderot.fr)

Accepted 12 July 2007
Journal of Cell Science 120, 3219-3227 Published by The Company of Biologists 2007
doi:10.1242/jcs.007492

Summary

The promyelocytic leukemia (PML) tumour suppressor is the organiser of PML nuclear bodies, which are domains the precise functions of which are still disputed. We show that upon several types of stress, endogenous PML proteins form nucleolar caps and eventually engulf nucleolar components. Only two specific PML splice variants (PML-I and PML-IV) are efficiently targeted to the nucleolus and the abundant PML-I isoform is required for the targeting of endogenous PML proteins to this organelle. We identified a nucleolar targeting domain within the evolutionarily conserved C-terminus of PML-I. This domain contains a predicted exonuclease III fold essential for the targeting of the PML-I C-terminus to nucleolar fibrillar centres. Furthermore, spontaneous or oncogene retrieval-induced senescence is associated with the formation of very large PML nuclear bodies that initially contain nucleolar components. Later, poly-ubiquitin conjugates are found on the outer shell or within most of these senescence-associated PML bodies. Thus, unexpectedly, the scarcely studied PML-I isoform links PML bodies, nucleolus, senescence and proteolysis.

Supplementary material available online at
http://jcs.biologists.org/cgi/content/full/120/18/3219/DC1

Key words: PML, Isoforms, Stress, Senescence, Proteasome, Nucleolus, Ubiquitin

Introduction

The human gene *PML* (promyelocytic leukemia) was identified as the fusion partner of *RARA* (retinoic acid receptor α) gene by the t(15;17) chromosomal translocation found in acute promyelocytic leukemia (APL) (de Thé et al., 1991). *PML* is composed of nine exons of which exons 5-9 can splice alternatively, yielding a large number of isoforms (Jensen et al., 2001). A TRIM motif (tripartite motif), also called RBCC (RING finger, B-box, coiled-coil), and encoded by exons 1-3, is present in all PML isoforms (Reymond et al., 2001) and is associated with E3 ubiquitin ligase activity for several other TRIM/RBCC proteins (Meroni and Diez-Roux, 2005; Urano et al., 2002). Alternative splicing of the C-terminal part of PML is likely to be important, because virtually all other TRIM/RBCC proteins display well-characterised functional domains in their C-terminus (Jensen et al., 2001; Short and Cox, 2006). The transcript encoding PML-I is highly expressed in normal cells and the corresponding protein accounts for the bulk of PML isoforms (Condemine et al., 2006). Several motifs have been identified in the C-terminus of PML: a nuclear localization signal (nls) and a SUMO-interacting motif (SIM) in all nuclear isoforms, and a nuclear exclusion signal (NES) in PML-I (Henderson and Eleftheriou, 2000), whereas PML-IV harbours binding motifs for p53 (Fogal et al., 2000; Guo et al., 2000) and HDM2 (Bernardi et al., 2004).

Nuclear matrix-bound PML proteins are organised in nuclear structures, called PML nuclear bodies (Daniel et al., 1993; Maul et al., 2000; Salomoni and Pandolfi, 2002). These bodies, which recruit a wide variety of otherwise unrelated proteins, have been tentatively associated with many functions, including transcription, protein degradation and DNA repair (Borden, 2002; Lallemand-Breitenbach et al., 2001; Wang et al., 1998; Nabetani et al., 2004). The formation of PML bodies relies on non-covalent interactions between SUMO-conjugated proteins, the SUMO-interacting motif of PML and the strong, coiled-coil-mediated, homo/multi-dimerization of PML (Lallemand-Breitenbach et al., 2001; Shen et al., 2006). Hence, most nuclear body-associated proteins are sumoylated, but what the functional consequence is of their transient association with PML and nuclear bodies (sequestration, modification, degradation…) is still disputed. Typical PML nuclear bodies are small spheres of 0.2-0.5 μm diameter. Larger PML bodies, called APB (alternative PML bodies), have been found in telomerase-negative cells and are presumed to be sites where telomeres are extended by homologous recombination (Henson et al., 2002; Yeager et al., 1999). APBs contain proteins such as MRE11, Nbs1 and Brca1, not found in typical nuclear bodies (Nabetani et al., 2004; Wu et al., 2000). More recently, 'giant' PML bodies were described in lymphocytes of patients with immunodeficiency, centromeric instability and facial dysmorphy (ICF) syndrome (Luciani et al., 2006). These bodies are very large protein structures generated during G2 phase which contain repair proteins. Morphologically distinct PML nuclear bodies were observed when *Pml*$^{-/-}$ MEFs over-express specific PML isoforms (Condemine et al., 2006), implying that the isoform-specific C-termini are in contact with nuclear components that influence morphogenesis of the bodies. Finally, PML nuclear bodies are rapidly altered by a wide variety of stresses such as virus infection, heat shock or exposure to DNA damage

(Dellaire and Bazett-Jones, 2004; Eskiw et al., 2003; Everett, 2006).

The nucleolus, essentially known as the site of transcription and maturation of ribosomal RNA, has three major compartments initially identified by electron microscopy. The fibrillar centre (FC) consists of fibrils of 50 Å diameter and contains the transcriptional factor UBF (upstream binding factor). The dense fibrillar compartment (DFC), which engulfs the fibrillar centre, is characterised by dense fibrils and the presence of fibrillarin, an RNA methyltransferase. The granular compartment (GC) is the site of partial maturation and assembly of pre-ribosomes and it accumulates nucleophosmin (NPM or B23), a protein implicated in oncogenesis (Kurki et al., 2004). Apart from ribosome biogenesis, the nucleolus was also implicated in a growing number of other functions, such as intra-nuclear traffic, chromatin assembly, biogenesis of other riboprotein particles and control of the cell cycle, possibly mediated by new nucleolar territories (Politz et al., 2005).

Previous studies had identified some connections between PML and the nucleolus (Bernardi et al., 2004; Mattsson et al., 2001), yet, the isoform dependence and the molecular mechanisms involved remained unclear. We show that nucleolar targeting of endogenous PML is specifically inhibited by extinction of the abundant PML-I isoform. We identify within this highly evolutionary conserved PML isoform a C-terminal domain that enable nucleolar targeting of GFP fusion protein. Finally, we identify, in senescent cells, very large nuclear PML bodies that contain either nucleolus components, poly-ubiquitin conjugates or both. Our findings shed new light on PML isoforms and their putative function and link PML to the nucleolus, senescence and proteolysis.

Results

Several types of stress induce targeting of endogenous PML to the nucleolus

When MRC5 primary fibroblasts, which express all PML isoforms, were irradiated with UV-C, nuclear bodies dispersed throughout the nucleus, and nucleolar necklaces could be observed, as recently described (Boe et al., 2006; Seker et al., 2003; Shav-Tal et al., 2005) (Fig. 1A and data not shown). Similarly, following treatment with doxorubicin (a topoisomerase II inhibitor) or actinomycin D (an RNA polymerase I inhibitor), endogenous PML formed nucleolar caps (Fig. 1A) (Bernardi et al., 2004). PML was also associated with the segregated nucleolar components following treatment with the proteasome inhibitor MG132 (Fig. 1B, data not shown) (Mattsson et al., 2001). Finally, when cells were irradiated with ionizing radiation γ (IR-γ), PML formed a few large, hollow nuclear bodies, which contained various nucleolar components, such as B23, fibrillarin and UBF, in addition to the classical bodies (Fig. 1A). Thus, endogenous PML proteins become associated with nucleolar components upon a wide variety of stress signals, although the exact topology (capping, engulfment, binding to segregated components…) may vary with the type of stress.

Stress-induced localization of specific PML isoforms

We then wondered whether the observed localization patterns of endogenous PML proteins upon stress might be specific for a given PML isoform. We thus transduced primary *Pml*$^{-/-}$ MEFs with retroviral vectors encoding the five major PML isoforms (I-V). Overall, the relative levels of PML proteins in these transduced cells mimicked those found in vivo (PML-I/II>PML-IV/V>PML-III) (Condemine et al., 2006), suggesting that a significant part of PML regulation is mediated by protein stability, dependent on the isoform-specific C-terminal regions (supplementary material Fig. S1A). In contrast to basal conditions, upon treatment with MG132, PML became associated with a compartment of segregated nucleolus, independently of the isoform expressed (supplementary material Fig. S1B,C, and Fig. 1B). However, while this was seen in all PML-IV-expressing cells and in over half of the cells expressing PML-I, it was only occasionally observed with other isoforms.

Following IR-γ, PML-I and -IV formed larger, hollow nuclear bodies that contained all nucleolar elements, in addition to classic nuclear bodies (Fig. 1A, and supplementary material Fig. S1D). This was observed in over 20% of the cells. In rare cases, PML-V also formed similar nucleolus-associated bodies, but PML-II and -III never showed modified nuclear bodies after irradiation. Essentially identical results were obtained upon administration of doxorubicin, although in that case, nucleolus-associated PML bodies were observed in over 50% of cells transduced with PML-I or -IV (supplementary material Fig. S1E). Finally UVC exposure lead to the dispersion of all PML isoforms as thousands of nucleoplasmic micro-dots, in virtually all cells (supplementary material Fig. S1F). Altogether, PML-I and -IV appear to be preferentially targeted to the periphery of the nucleolus in response to genotoxic stress, whereas all isoforms associate with nucleolar components upon inhibition of proteolysis, pointing to distinct pathways or partners involved in stress-induced PML nucleolar localization.

We have previously shown that all PML isoforms colocalise, reflecting their ability to heterodimerise, and that PML-I is the most abundantly expressed one (Condemine et al., 2006). Given that PML-I is abundant and efficiently targeted to the nucleolus in response to genotoxic stress, we wondered whether endogenous PML isoforms would still exhibit nucleolar targeting in response to genotoxic stress after the specific extinction of PML-I. We thus designed a siRNA selectively targeting the PML-I isoform, which indeed abolished the PML-I expression only. In these PML-I-depleted cells, the perinucleolar targeting of PML upon doxorubicin exposure was lost compared to a non-relevant siRNA (Fig. 1C). By contrast, nucleolar targeting of endogenous PML upon inhibition of proteolysis was unaffected by extinction of PML-I (data not shown). This experiment therefore demonstrates that the perinucleolar targeting of endogenous PML isoforms upon doxorubicin exposure is largely dependent on the expression of PML-I (Fig. 1C), PML-IV probably being too scarce to drive other abundant isoforms such as PML-II to this organelle. By contrast, proteasome-inhibition triggered recruitment of PML to a specific compartment of disrupted nucleoli shows little isoform specificity, again implying that its mechanism is distinct.

Nucleolar targeting of PML-I C-terminus

PML-I has the largest C-terminus of all PML isoforms (Condemine et al., 2006). Comparing the sequence of this region in various organisms (*Homo sapiens*, *Pan trogloides*,

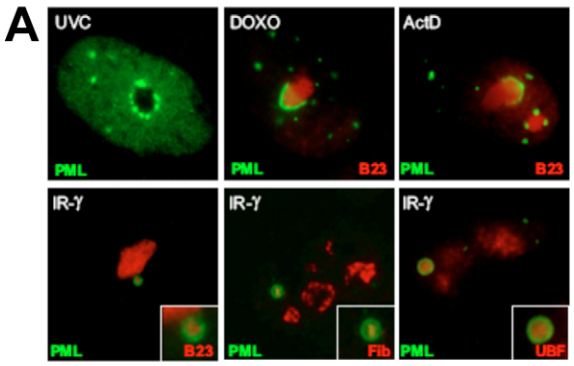

B

	Localization pattern	Preferentially relocalized isoforms
MG132	Nucleolus	+/- I, IV
IR-γ	Large hollow NB's	Strictly I, IV (V)
Doxo	Large hollow NB's	+/- I, IV
UVC	Dispersed	None

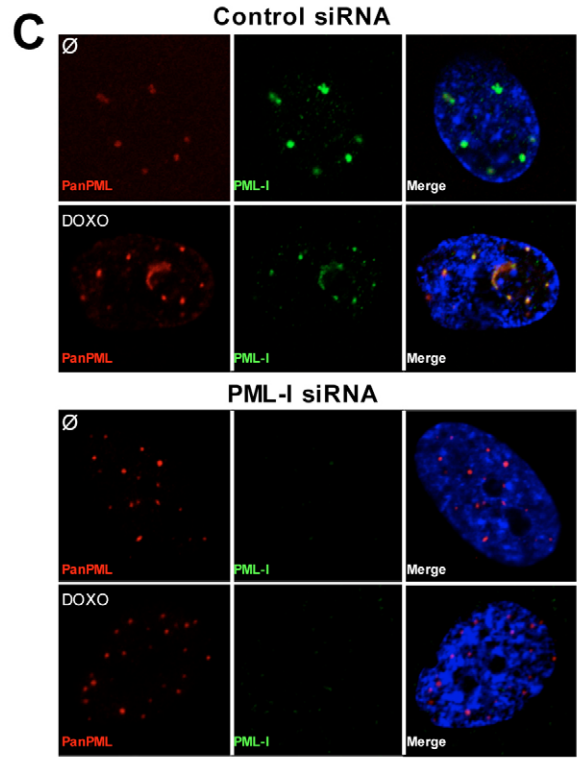

Fig. 1. (A,B) PML is targeted to the nucleolus upon cellular stresses. Confocal images of MRC5 human fibroblasts treated with 35 J/m^2 UVC radiation (1 hour), 2 μg/ml doxorubicin (Doxo) for 24 hours, 5 nM actinomycin D (ActD) for 16 hours, 10 μM MG132 for 16 hours, or 10 Gy ionizing radiation γ (IR-γ) (1 hour). Immunofluorescence was performed using antibodies against PML, B23, fibrillarin or UBF, as indicated. (B) Summary of the localization patterns observed in *Pml*$^{-/-}$ MEFs expressing PML isoforms -I, -II, -III, -IV or -V, and treated as indicated. NBs, nuclear bodies. (C) PML-I targets nucleolar caps upon doxorubicin treatment. MRC5 cells were transfected with PML-I specific or control siRNA and treated with doxorubicin for 24 hours. Immunofluorescence was then performed using Pan-PML or PML-I-specific sera, as indicated. Nuclei were stained with DAPI.

Mus musculus, *Rattus norvegicus*, *Bos taurus*, *Gallus gallus*, *Canis familiaris*, *Felix catus*, *Sus scrofa*, *Loxodonta africana*, and others) we found an unexpected level of sequence conservation throughout the sequence (supplementary material Fig. S2A). Computer based domain prediction analysis of the PML-I C-terminus identified a putative exonuclease-III-like motif between residues 610 and 759, in most organisms. This exonuclease type III (Exo-III) domain belongs to the most conserved protein blocks, although regions C-terminal to the Exo-III domain were also highly conserved (supplementary material Figs S2, S3). Attempts to demonstrate nucleic acid binding or DNase and/or RNase activities have been unsuccessful to date (data not shown).

To further characterise the properties of PML-I C-terminus, we studied the intracellular localization of the complete 607-882 PML-I C-terminus fused to a nls-GFP tag. When transiently overexpressed in SaOS, COS, CHO or *Pml*$^{-/-}$ MEFs, the fusion protein was very efficiently targeted to the nucleolus (Fig. 2A and data not shown). The three compartments of the nucleolus were targeted by the fusion protein, as shown by colocalization with proteins such as UBF, fibrillarin or B23 and RNA. Yet, importantly, UBF dots displayed a very significant enhancement in the accumulation of the GFP-PML C-terminus fusion protein, when compared to the rest of the nucleolus (Fig. 2A). Loss of the last 16 residues of this PML-I C-terminus-GFP fusion protein resulted in the disappearance of UBF-colocalizing dots, but not of the diffuse signal (Fig. 2B and data not shown). These 16 residues, although not conserved between mouse and human, are significantly conserved between human and several other species (supplementary material Fig. S2). Conversely, deletion of the very first N-terminal residues (607-619) of the putative Exo-III domain resulted in loss of the nucleolar localization. Altogether, these observations strongly suggests that the highly folded putative Exo-III domain is critical for the proper targeting of the fusion, but that more C-terminal sequences are also required, particularly for its accumulation on the fibrillar centre.

PML-IV and PML-I share a short common C-terminal sequence encoded by exon 8a, which constitutes the N-terminal part of the Exo-III domain. When fused to GFP, the full-size PML-IV C-terminus (607-633) also conferred nucleolar targeting (Fig. 2C). The PML-IV-specific C-terminal 12 amino acids (encoded by exon 8b) failed to do so, whereas the first 11 amino acids of the Exo-III domain sufficed to confer nucleolar targeting to GFP (data not shown). Curiously, nucleolar targeting was also observed with GFP fusions involving the PML-V C-terminus (571-611), encoded by the exon 7ab (Fig. 2D), despite the absence of any common sequence with PML-I or PML-IV (Fig. 2E). No specific intra-nuclear patterns were observed with PML-II and PML-III C-terminus. In contrast to the 275 amino-acid sequence of PML-I C-terminus, which probably contains one or several protein

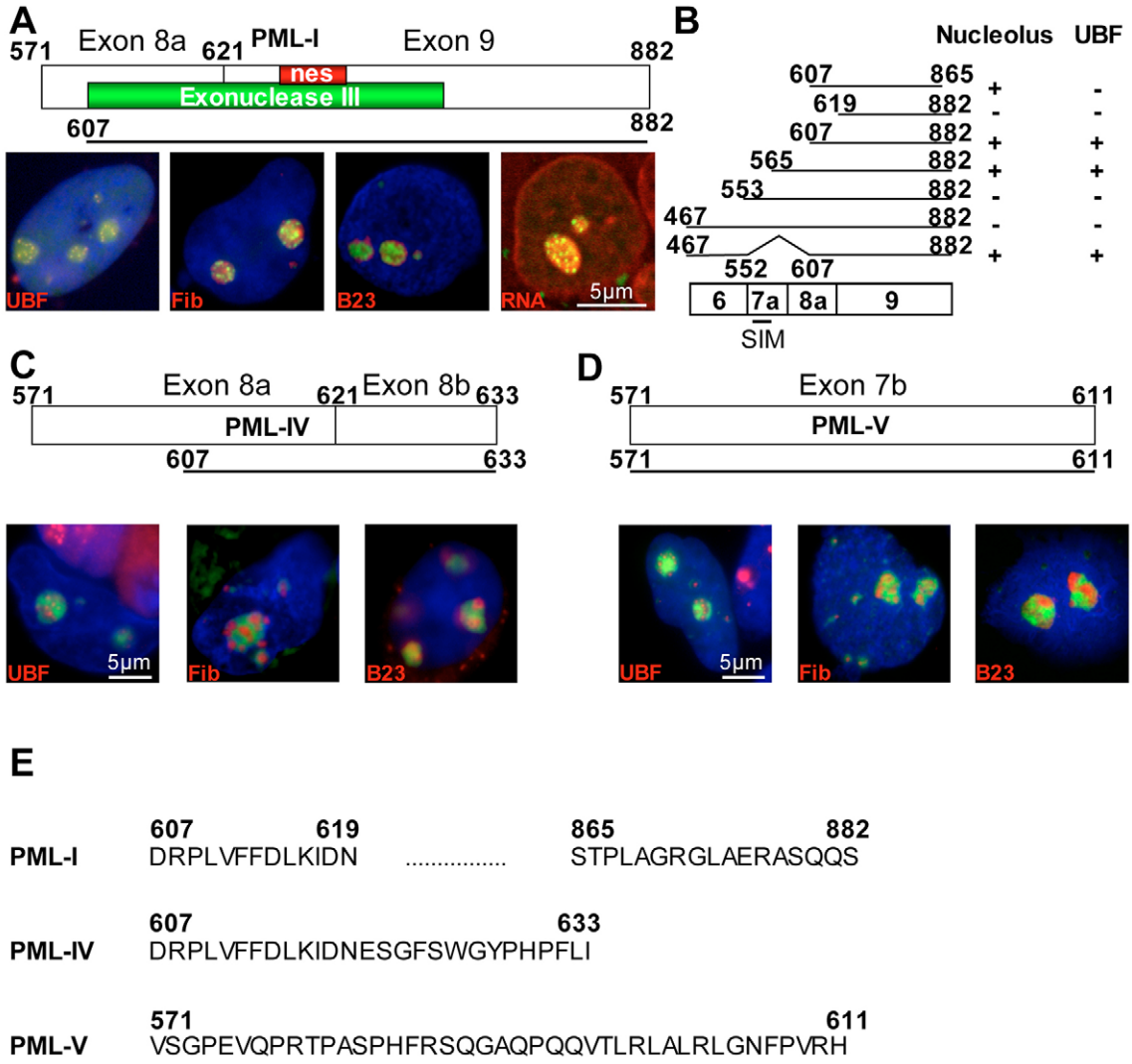

Fig. 2. Specific PML isoform C-terminus encodes a nucleolar targeting domain. (A) Plasmids encoding the various nls-GFP fusion proteins (top) were transfected into human osteosarcoma cells, SaOS, which were observed 24 hours later. GFP-PML fusion proteins appear in green, nucleolar markers UBF, fibrillarin, B23 and RNA (revealed by BET), in red. (B) The presence of a inhibitor domain SIM in the C-terminus of PML-I. Different PML-I C-terminal fragments are fused to nls-GFP to estimate their nucleolar targeting property. Results are reported in the diagram. (C,D) Characterization of the targeting of the PML-IV-specific terminus (C) and the PML-V-specific terminus (D). The PML sequence is indicated by the positions of the residues on the original isoforms. Staining as in A. (E) Amino acid sequences of the regions required for nucleolar association in PML-I (607-619 and 865-882), PML-IV (607-633) and PML-V (571- 611).

folds, fusion of these short peptides to GFP should be interpreted with caution. Altogether, nucleolar targeting is a property shared by the three evolutionarily conserved C-termini of PML isoforms I, IV and V, but the highly specific UBF localization is a specific feature of PML-I C-terminus.

We examined the effect of deletion of these nucleolar-targeting domains identified above on PML localization upon doxorubicin exposure. Importantly, when the PML core common to all isoforms (1-552) was stably expressed in *Pml*$^{-/-}$ cells and exposed to doxorubicin, formation of nucleolar caps was no longer observed (see supplementary material Fig. S1G). Deletions within the Exo-III domain of the PML-I isoform did not yield interpretable results, as they induced protein instability, possibly because of misfolding. Altogether, these experiments strongly suggest that endogenous PML isoforms are addressed to the nucleolus upon stress through their oligomerization with PML-I, whose C-terminal domain contains a potent nucleolar-targeting signal.

Inhibition of nucleolar targeting by the PML SIM motif

We then expressed a set of PML-I C-terminus GFP fusions which were progressively extended towards the N-terminal coiled-coil. Unexpectedly, loss of nucleolar targeting was observed as soon as the complete exon 7a was present in the constructs (Fig. 2B). Conversely, when region 552-607 encoded by exon 7a, which includes the SUMO interacting motif (SIM), was deleted from the 467-882 fusion, nucleolar targeting was fully restored (Fig. 2B). This observation strongly suggests an inhibitory function of SIM on the nucleolar targeting of PML-I C-terminus. The PML-I C-

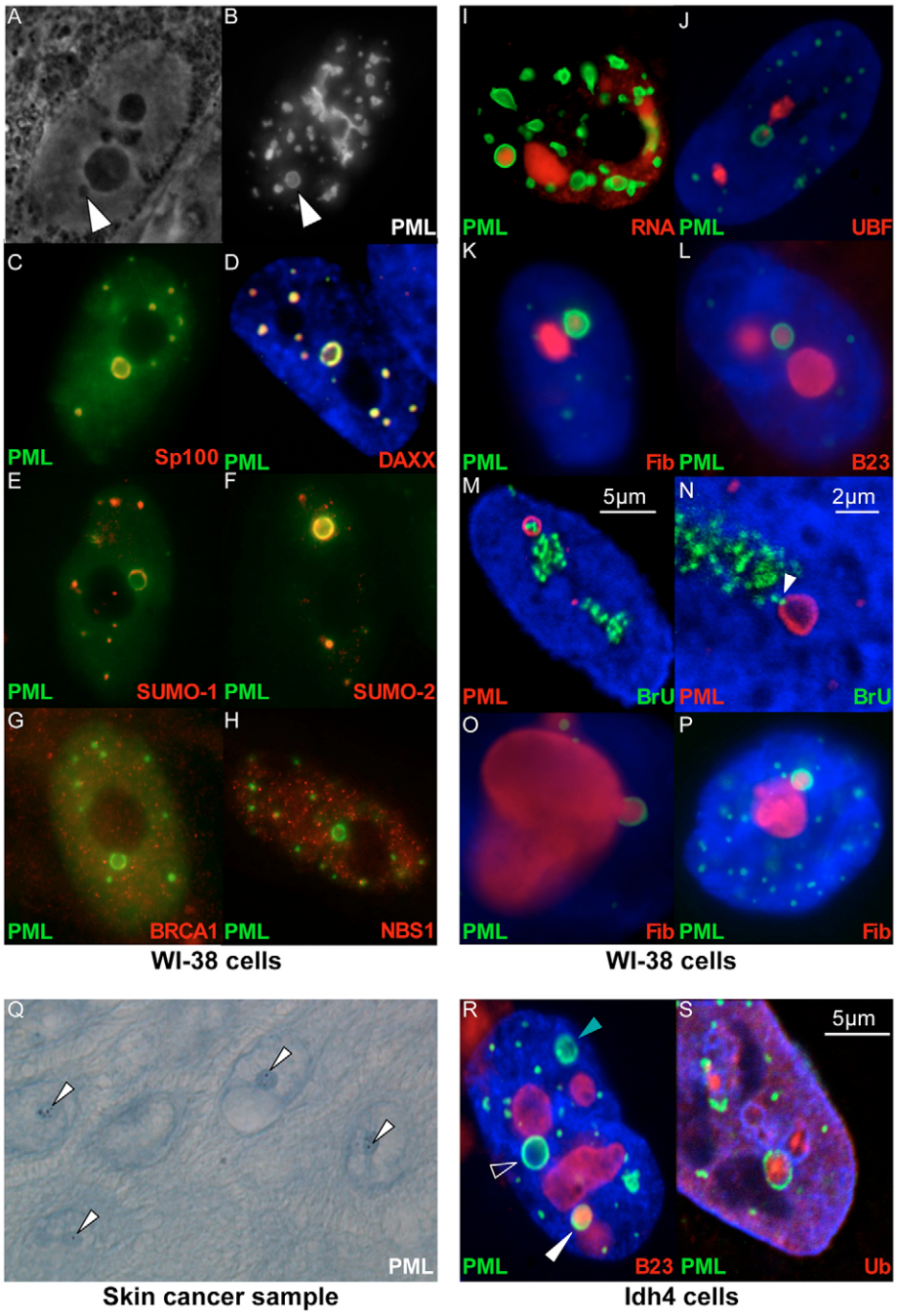

Fig. 3. Characterization of nucleolus-associated PML structures. (A-H) Senescence-associated nuclear bodies. (A,B) Phase contrast images of WI-38 cells transduced with GFP-PML-I (see Movie 1 in supplementary material). (C-H) Untransfected WI-38 cells labelled for the following proteins: PML (green) or Sp100, DAXX, SUMO-1 and 2, Brca1 and Nbs1 (red). (I-P) Nucleolar components in SANB. (I-L) PML (green). RNA, UBF, Fibrillarin and B23 appear in red. (M,N) RNA pol I associated transcriptional activity in SANB. PML appears red and BrU green. (O,P) PML budding structures from the nucleolus. PML appears green and the nucleolus (fibrillarin) red. (Q) Biopsies from skin cancers were analysed with PML antisera. PML localises in the nucleolus (white arrow). (R,S) Senescent Idh4 cells exhibit SANB-like bodies. PML (green) and B23 or ubiquitin (red). White filled arrowhead, SANB-containing nucleolar components; open and green arrowheads, nucleolar-free SANB not in contact with nucleolus. All the images were obtained using photon microscopy, except images M-N and S, which were obtained with confocal microscopy.

terminus contains a previously unidentified consensus sumoylation site that may contribute to nucleolus interactions but be auto-inhibited by the SIM domain, as well-documented for ubiquitin and ubiquitin-binding domains (Hoeller et al., 2006). Deletion of the SIM domain, which was implicated in PML instability upon CK2 activation (Scaglioni et al., 2006), did not alter the localization of the full-length PML protein to nuclear bodies (Shen et al., 2006) (data not shown).

Senescence targets PML to the nucleolus

Unstressed WI-38 human primary fibroblasts occasionally show, in addition to classical PML nuclear bodies, large spheres of 2-3 μm diameter, surrounded by a very thin PML shell, often visible in phase contrast microscopy (Fig. 3A,B). Traditional components of PML nuclear bodies (Sp100, Daxx, SUMO-1, SUMO-2) all colocalised with PML on the shell of these bodies (Fig. 3C,D,E,F), but none of the typical APB proteins (Brca1, Nbs1) were ever detected (Fig. 3G,H). These PML domains are often in close proximity to, or in direct contact with, the nucleolus, and to some extent resemble the ones observed upon genotoxic stresses (Fig. 1A).

We thus investigated the presence of nucleolar elements in this subtype of PML bodies and indeed found UBF, fibrillarin, B23 and RNA (Fig. 3I,J,K,L) and sometimes Ki-67 (data not shown) in most of them. RNA polymerase I-associated transcriptional activity (detected by BrU incorporation) was

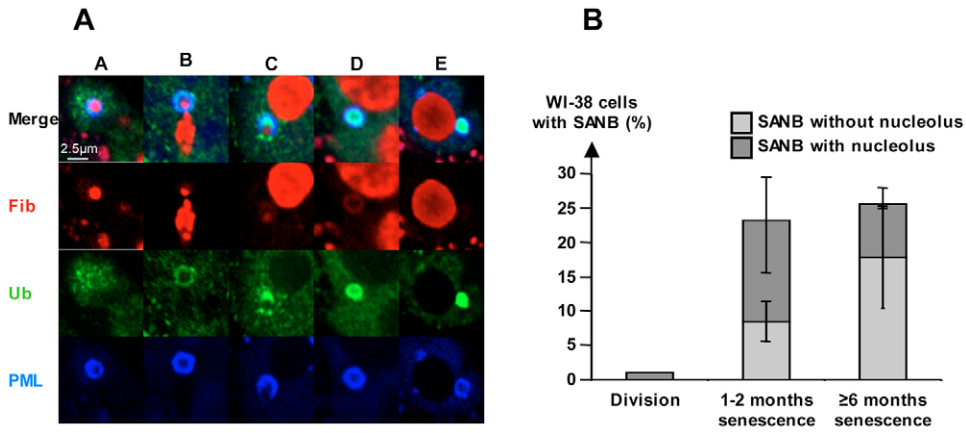

Fig. 4. SANB composition varies with the advancement of senescence. (A) Progression of senescence [dividing cells (A) to late senescent cells (E)] is associated with a decrease in the nucleolar component, fibrillarin, but an increase in poly-ubiquitin conjugates. Fibrillarin is red, ubiquitin appears green and PML blue. (B) Bar graph representing the percentage of WI-38 cells with SANB depending on the state (dividing/senescent) of the cells. The columns represent the average of three independent experiments.

detected in a sub-population of these bodies (Fig. 3M,N). Interestingly, in some cases, the BrU signal colocalised with the discontinuity in the PML shell, which may correspond to the passage of chromosomes through the PML shell (Fig. 3M,N). In some images of these WI-38 cells, PML is associated with a bud, seemingly emerging from the nucleolus (Fig. 3O,P). To further establish this PML-nucleolus link in vivo, we performed immunohistochemistry on human tumours and indeed found that in several skin tumours, PML staining was associated with the nucleolus (Fig. 3Q).

In WI-38 cells, progression towards senescence was associated with a sharp increase in the abundance of these large PML bodies (see Fig. 4B below). In Idh4 cells, which conditionally express the SV40T oncogene, loss of SV40T expression induces senescence and changes in the morphology of PML bodies (Jiang et al., 1996; Jiang and Ringertz, 1997). In oncogene-deprived senescent Idh4 cells, as above in WI-38 cells, PML, Daxx, Sp100 and SUMO usually labelled the outer shell, whereas fibrillarin, B23 and UBF stained the inner part of the structure (Fig. 3R,S, data not shown). To address the possibility that formation of these bodies might reflect a change in the isoform composition of endogenous PML proteins, we analysed dividing or senescent WI-38 cells and Idh4 cells expressing, or not, SV40T, by western blotting. No significant changes in isoform expression were observed with a pan-PML antibody (data not shown). We then attempted to inactivate PML-I by siRNA, as above, but could never significantly decrease PML-I expression in WI-38 cells undergoing spontaneous senescence, precluding the demonstration of a direct implication of PML-I in the perinucleolar targeting of PML during senescence. Altogether, in two different cellular models, senescence is associated with the formation of very large PML bodies containing a nucleolar element, for which we propose the name senescence-associated nuclear bodies (SANB).

Many senescence-associated nuclear bodies stain for poly-ubiquitin

Several studies have reported the presence of some proteasome components on PML bodies upon expression of misfolded proteins or arsenic exposure (Anton et al., 1999; Lafarga et al., 2002; Lallemand-Breitenbach et al., 2001). We detected poly-ubiquitin conjugates in most SANB observed in Idh4 and WI-38 cells (Fig. 3S, Fig. 4A). Interestingly, in SANB, poly-ubiquitin staining appeared to be inversely related to the detection of nucleolar components and to senescence progression (Fig. 4B). In pre-senescent cells, most SANB show significant staining for fibrillarin, but little or none for poly-ubiquitin (Fig. 4A, column A). In senescent cells, poly-ubiquitin either colocalised with the PML shell (Fig. 4A, column B) or was present within SANB (Fig. 4A, columns C, D), with some remaining nucleolar components. Finally, PML shells with a strongly poly-ubiquitin-positive inner mass were found in terminally senescent cells (Fig. 4A, column E). Large PML bodies with neither poly-ubiquitin nor nucleolar component were also occasionally observed (data not shown).

When dividing WI-38 cells were treated with the proteasome inhibitor MG132 for 2 hours, poly-ubiquitin staining appeared on most normal PML bodies (Fig. 5). When these cells were exposed to the nuclear export inhibitor leptomycin B (LMB), poly-ubiquitin stained bodies appeared adjacent to each PML nuclear body, as previously shown (Lain et al., 1999). The association of MG132 and LMB essentially yielded the staining patterns observed with MG132, but, curiously, in a small number of cells, poly-ubiquitin bridges were regularly observed to link one PML body to another (Fig. 5, lower panel).

Dynamic analysis of SANB

Because the images of budding suggested that SANB might be dynamic structures, and inhibition of nuclear export exerts dramatic effects on PML localization, WI-38 cells transduced by GFP-PML-I were examined using real-time videos. The level of expression of GFP-PML-I was modest, in the order of 10-20% of total PML (data not shown). In three independent observations, classical PML nuclear bodies were found to be highly mobile structures that divide or fuse with themselves (Dellaire et al., 2006), whereas SANB fuse with incoming classical nuclear bodies, but were never observed to divide or to bud from the nucleolus, suggesting that these domains are relatively stable (supplementary material Movie 1).

Discussion

In this report, we establish a strong relationship between PML and the nucleolus, provide mechanistic insights into its molecular basis and associate this process with senescence and proteolysis. Interestingly, other proteins involved in metabolism of ubiquitin-like proteins, such as the SUMO

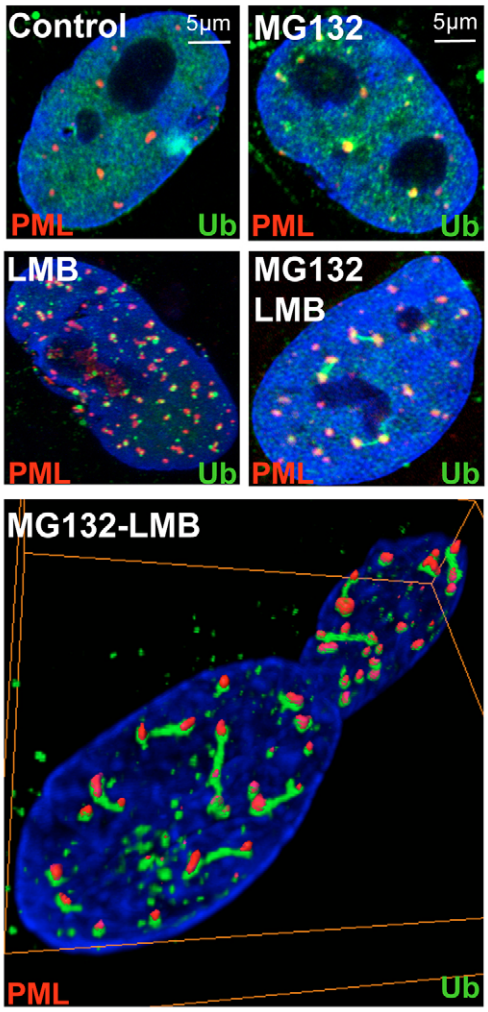

Fig. 5. Inhibitors link PML bodies to protein degradation and trafficking. Top four panels: Primary WI-38 cells were treated with either 10 μM MG132 or 1 μM LMB or both for 2 hours, allowing co-localization of ubiquitin (green) and PML (red). LMB panel is a *Z*-projection of a confocal stack acquisition. Bottom panel: 3D reconstruction of deconvoluted images.

protease SENP5 or the viral ubiquitin ligase ICP0, also shuttle between PML nuclear bodies and the nucleolus, depending on the cellular context (Gong and Yeh, 2006; Morency et al., 2005). Endogenous PML (Bernardi et al., 2004; Mattsson et al., 2001; Rokaeus et al., 2006) and three PML isoforms (PML-I, -IV and -V) are targeted to the nucleolus upon genotoxic stress (Fig. 1), most likely through the nucleolar targeting domains that we have identified. That the C-termini of these three isoforms are the only evolutionarily conserved ones (Condemine et al., 2006) is strongly suggestive for an important functional relationship between PML and the nucleolus. Identification of a critical domain C-terminal to the RBCC core was expected, as virtually all other RBCC/TRIM proteins exhibit one (Short and Cox, 2006) and computer based analysis of the PML-I C-terminal domain strongly predicts a globular folding and shows very high evolutionary conservation (supplementary material Fig. S2B and Fig. S3, and data not shown). Interestingly, this folded and conserved domain is the one mediating nucleolar targeting of GFP fusion. Yet, full-length PML proteins do not spontaneously accumulate in the nucleolus, implying that the RBCC moiety of the PML proteins counteract the intrinsic nucleolar targeting of the PML C-terminus. Several non-exclusive hypotheses could account for this finding. First, the RBCC domain, which is able to form nuclear bodies on its own (supplementary material Fig. S1G, and data not shown), has a strong nucleoplasmic anchor. Second, the PML C-termini may be systematically located inside the body or, in the context of the full-size protein, folded in a way that precludes contact. A last hypothesis could be that the full-length protein degrades the component that is targeted by the C-terminal region. The PML-I C-terminus specifically targets the fibrillar centre, yet two-hybrid screens failed to identify protein partner that could account for this nucleolus association (data not shown). The highly conserved Exo-III domain is required for addressing GFP to the nucleolus (data not shown) and it is possible that association with nucleic acids, such as polymerase I ribosomal RNAs, could be implicated in this targeting process. In that respect, polymerase II transcripts were previously observed in PML bodies (LaMorte et al., 1998).

We have identified in senescent cells a new type of PML body, SANB, clearly different from APB or giant bodies (Luciani et al., 2006), because of the absence of DNA repair proteins and of their presence in G0 and G1 phases of the cell cycle (data not shown). The outer shell of these large PML scaffolds also sometimes associates with sub-domains labelled with SUMO, ubiquitin or Sp100 (supplementary material Fig. S4). This new type of PML body exhibits a close relationship with the nucleolus and the ubiquitin proteasome pathway. The various combinations of ubiquitin and nucleolar components found in SANB (Fig. 4) could suggest the following sequential model: PML is first targeted to the nucleolar periphery, nucleolar elements bud from the nucleolus (Fig. 3O,P), SANB inner components undergo poly-ubiquitination and degradation, and finally, ubiquitin conjugates fill in the remaining structure. Previously, poly-ubiquitin and proteasome components have occasionally been observed in PML nuclear bodies during viral infection, arsenic treatment or overexpression of misfolded proteins (Anton et al., 1999; Everett, 2000; Lafarga et al., 2002; Lallemand-Breitenbach et al., 2001). In the primary WI-38 cells studied here, PML bodies appear to be tightly associated to the ubiquitin/proteasome system, as shown by the dramatic effect of a brief exposure to proteasome inhibitors to recruit/stabilise poly-ubiquitin onto nuclear bodies. Moreover, that poly-ubiquitin bridges linking adjacent nuclear bodies were observed in the presence of proteasome inhibitors and LMB (Fig. 5), might reflect the existence of physical links, possibly related to the nuclear matrix, between the different bodies.

In spontaneously senescent fibroblasts, PML is targeted to the nucleolus and proteasomal activity decreases, which may contribute to the accumulation of poly-ubiquitin within SANB (Fig. 4). Conversely, proteasome inhibition first recruits poly-ubiquitin onto PML bodies (Fig. 5), and later induces the targeting of PML to the nucleolus (Fig. 1A). Prolonged proteasome inhibition may also trigger senescence (Torres et al., 2006). PML-IV over-expression triggers senescence and *Pml*$^{-/-}$ cells fail to senesce upon expression of oncogenic Ras (Bischof et al., 2002; Pearson et al., 2000). Collectively, these

observations suggest that the nucleolar targeting of PML during senescence may not be a side-effect, but that PML could participate in the regulation of this process.

Materials and Methods

Cell-lines, transfection and treatment

Human osteosarcoma cells SaOS, Plat-E packaging cells, MRC5, mouse embryonic fibroblasts (MEFs) and human primary fibroblasts WI-38 were cultured in Dulbecco's modified Eagle's medium (Life Technologies, Grand Island, NY) supplemented with 10% fetal bovine serum, 50 IU/ml penicillin, 50 mg/ml streptomycin and 2 mM glutamine. Cells were transfected with the Effectene kit (Qiagen). Idh4 (a gift from Woodring E. Wright, UT Southwestern Medical Centre, Dallas, TX) were cultured in DMEM with 10% charcoil-depleted serum (iron-supplemented bovine serum; Perbio, Erembodegen, Belgium) and 5 μM dexamethasone. Senescence was induced by depletion of dexamethasone, as previously described (Jiang et al., 1996; Jiang and Ringertz, 1997). *Pml*$^{-/-}$ MEFs were obtained from 13- to 14-day mouse embryos. Plat-E packaging cells were transfected with retroviral vectors MSCV-PML-I, -II, -III, -IV or -V, using the calcium-phosphate method (Invitrogen). The supernatant containing the retrovirus was collected at 24 and 32 hours post-transfection, supplemented with 2 μg/μl polybrene (Sigma), and added to MEFs. Doxorubicin (Sigma), actinomycin D (Sigma) and MG132 (Calbiochem) were used at 0.1-2 μg/ml, 5 nM and 10 μM, respectively, for the indicated time period. For siRNA experiments, MRC5 cells were transfected in a 24-well plate with 40 ng of either siRNA duplex toward the following PML target sequence (5′-TGCGGTGAACCGGGAAGCAA-3′), or commercial siRNA control duplex toward GFP target sequence (5′-CGGC-AAGCTGACCCTGAAGTTCAT-3′, Qiagen) using HyperFect reagent (Qiagen), according to the manufacturer's instructions. Forty-eight to 72 hours later, cells were harvested for immunofluorescence characterization.

Immunofluorescence

Cells were cultured on 12 mm diameter coverslips. Fixation was performed using either 4% paraformaldehyde for 20 minutes at 4°C or room temperature, or methanol for 5 minutes at –20°C. Cells were permeabilised with PBS-0.1% Triton X-100, either before or after fixation. PML was labelled with either 5E10, a murine antibody directed against a common region for all the isoforms (Koken et al., 1994), or with rabbit sera or chicken sera generated in the laboratory (Pan-PML- and PML-I-specific serum) (Condemine et al., 2006). Ubiquitin was detected using the monoclonal antibody FK2 (Biomol International, Plymouth Meeting, PA). B23 antibody was obtained from Santa Cruz Biotechnology. Antisera directed against UBF and fibrillarin were gifts from D. Hernandez-Verdun, UMR 7592, Paris, France. Bound antibodies were labelled with Alexa Fluor 488- (Molecular Probes), Alexa Fluor 594- (Molecular Probes), or AMCA- (Jackson ImmunoResearch) conjugated secondary antibodies for 1 hour and mounted with VectaShield ± DAPI (Vector). Observations were made either by confocal microscopy LSM510META (Zeiss; 63× NA 1.4 oil immersion lens) or by photon microscopy or 4-5D videomicroscopy (Institute Curie, Paris). Images from confocal microscopy were deconvoluted with AutoDeblur Software (AutoQuant Imaging Inc., Troy, NY). Three-dimensional reconstructions were performed with Amira 4.0 Software (Mercury Computer Systems, Chelmsford, MA).

Run-on experiment

Cells grown on coverslips were rinsed in PBS, fixed in methanol for 1 minute at –20°C, permeabilised with 0.1% Triton X-100 in PBS for 1 minute, equilibrated in transcription buffer (TB: 100 mM KCl, 5 mM $MgCl_2$, 0.5 mM EGTA, 5 IU/ml RNAsin, 25% glycerol and 50 mM Tris-HCl, pH 7.4) and incubated for 1 hour at 37°C in TB containing 0.5 mM rATP, 0.5 mM rCTP, 0.5 mM rGTP and 0.5 mM bromo-uridine (BrU). After rinsing in PBS and a second fixation in methanol for 5 minutes at –20°C, BrU was detected with the monoclonal antibody BMC9318 (Roche).

Clinical samples

Stored paraffin blocks of surgical samples removed for diagnostic procedures were used in this study, after the diagnostic had been fully established. Patients were informed of the study according to the Institution's regulations. Sequential 5 μm thick sections were made on a microtome with water flow (HM 350 Niagara, Microm France). An indirect immunoperoxidase staining method was used, on a Ventana Nexes automate, with a pan-PML primary antibody at a 1:100 dilution without antigen retrieval.

We thank Danielle Hernandez-Verdun for the gift of anti-sera directed against human UBF and fibrillarin, and for her helpful advice and comments on the manuscript, and Woodring E. Wright for his kind gift of Idh4 cells. We thank Anne-Marie Poorters for the sequencing of constructs. We are also grateful to Frédéric Brau, Michel Schmidt, Micaël Yagello and Niclas Setterblad at the Service Commun d'Imagerie of the IUH of Saint-Louis Hospital for the confocal microscopy, as well as Geneviève Almouzni and Patricia Le Baccon at Institut Curie UMR 218 for the video microscopy. W.C. had a scholarship from ARC and MRT, as well as Virus Cancer Prevention. Y.T. had a scholarship from MAE and ARC. M.L.B. had a fellowship from EU. These data were presented at the Cold Spring Harbor Symposium 'Dynamic Organization of the Nucleus' in September 2004.

References

Anton, L. C., Schubert, U., Bacik, I., Princiotta, M. F., Wearsch, P. A., Gibbs, J., Day, P., Realini, C., Rechsteiner, M., Bennink, J. et al. (1999). Intracellular localization of proteasomal degradation of a viral antigen. *J. Cell Biol.* **146**, 113-124.

Bernardi, R., Scaglioni, P. P., Bergmann, S., Horn, H. F., Vousden, K. H. and Pandolfi, P. P. (2004). PML regulates p53 stability by sequestering Mdm2 to the nucleolus. *Nat. Cell Biol.* **6**, 665-672.

Bischof, O., Kirsh, O., Pearson, M., Itahana, K., Pelicci, P. G. and Dejean, A. (2002). Deconstructing PML-induced premature senescence. *EMBO J.* **21**, 3358-3369.

Boe, S. O., Haave, M., Jul-Larsen, A., Grudic, A., Bjerkvig, R. and Lonning, P. E. (2006). Promyelocytic leukemia nuclear bodies are predetermined processing sites for damaged DNA. *J. Cell Sci.* **119**, 3284-3295.

Borden, K. L. (2002). Pondering the promyelocytic leukemia protein (PML) puzzle: possible functions for PML nuclear bodies. *Mol. Cell. Biol.* **22**, 5259-5269.

Condemine, W., Takahashi, Y., Zhu, J., Puvion-Dutilleul, F., Guegan, S., Janin, A. and de The, H. (2006). Characterization of endogenous human promyelocytic leukemia isoforms. *Cancer Res.* **66**, 6192-6198.

Daniel, M.-T., Koken, M., Romagné, O., Barbey, S., Bazarbachi, A., Stadler, M., Guillemin, M.-C., Degos, L., Chomienne, C. and de Thé, H. (1993). PML protein expression in hematopoietic and acute promyelocytic leukemia cells. *Blood* **82**, 1858-1867.

de Thé, H., Lavau, C., Marchio, A., Chomienne, C., Degos, L. and Dejean, A. (1991). The PML-RAR alpha fusion mRNA generated by the t(15;17) translocation in acute promyelocytic leukemia encodes a functionally altered RAR. *Cell* **66**, 675-684.

Dellaire, G. and Bazett-Jones, D. P. (2004). PML nuclear bodies: dynamic sensors of DNA damage and cellular stress. *BioEssays* **26**, 963-977.

Dellaire, G., Ching, R. W., Dehghani, H., Ren, Y. and Bazett-Jones, D. P. (2006). The number of PML nuclear bodies increases in early S phase by a fission mechanism. *J. Cell Sci.* **119**, 1026-1033.

Eskiw, C. H., Dellaire, G., Mymryk, J. S. and Bazett-Jones, D. P. (2003). Size, position and dynamic behavior of PML nuclear bodies following cell stress as a paradigm for supramolecular trafficking and assembly. *J. Cell Sci.* **116**, 4455-4466.

Everett, R. D. (2000). ICP0 induces the accumulation of colocalizing conjugated ubiquitin. *J. Virol.* **74**, 9994-10005.

Everett, R. D. (2006). Interactions between DNA viruses, ND10 and the DNA damage response. *Cell. Microbiol.* **8**, 365-374.

Fogal, V., Gostissa, M., Sandy, P., Zacchi, P., Sternsdorf, T., Jensen, K., Pandolfi, P. P., Will, H., Schneider, C. and Del Sal, G. (2000). Regulation of p53 activity in nuclear bodies by a specific PML isoform. *EMBO J.* **19**, 6185-6195.

Gong, L. and Yeh, E. T. (2006). Characterization of a family of nucleolar SUMO-specific proteases with preference for SUMO-2 or SUMO-3. *J. Biol. Chem.* **281**, 15869-15877.

Guo, A., Salomoni, P., Luo, J., Shih, A., Zhong, S., Gu, W. and Paolo Pandolfi, P. (2000). The function of PML in p53-dependent apoptosis. *Nat. Cell Biol.* **2**, 730-736.

Henderson, B. R. and Eleftheriou, A. (2000). A comparison of the activity, sequence specificity, and CRM1-dependence of different nuclear export signals. *Exp. Cell Res.* **256**, 213-224.

Henson, J. D., Neumann, A. A., Yeager, T. R. and Reddel, R. R. (2002). Alternative lengthening of telomeres in mammalian cells. *Oncogene* **21**, 598-610.

Hoeller, D., Crosetto, N., Blagoev, B., Raiborg, C., Tikkanen, R., Wagner, S., Kowanetz, K., Breitling, R., Mann, M., Stenmark, H. and Dikic, I. (2006) Regulation of ubiquitin-binding proteins by monoubiquitination. *Nat. Cell Biol.* **8**, 163-169

Jensen, K., Shiels, C. and Freemont, P. S. (2001). PML protein isoforms and the RBCC/TRIM motif. *Oncogene* **20**, 7223-7233.

Jiang, W. Q. and Ringertz, N. (1997). Altered distribution of the promyelocytic leukemia-associated protein is associated with cellular senescence. *Cell Growth Differ.* **8**, 513-522.

Jiang, W.-Q., Szekely, L., Klein, G. and Ringertz, N. (1996). Intranuclear redistribution of SV40T, p53, and PML in a conditionally SV40T-immortalized cell line. *Exp. Cell Res.* **229**, 289-300.

Koken, M. H. M., Puvion-Dutilleul, F., Guillemin, M. C., Viron, A., Linares-Cruz, G., Stuurman, N., de Jong, L., Szostecki, C., Calvo, F., Chomienne, C. et al. (1994). The t(15;17) translocation alters a nuclear body in a RA-reversible fashion. *EMBO J.* **13**, 1073-1083.

Kurki, S., Peltonen, K., Latonen, L., Kiviharju, T. M., Ojala, P. M., Meek, D. and Laiho, M. (2004). Nucleolar protein NPM interacts with HDM2 and protects tumor suppressor protein p53 from HDM2-mediated degradation. *Cancer Cell* **5**, 465-475.

Lafarga, M., Berciano, M. T., Pena, E., Mayo, I., Castano, J. G., Bohmann, D., Rodrigues, J. P., Tavanez, J. P. and Carmo-Fonseca, M. (2002). Clastosome: a subtype of nuclear body enriched in 19S and 20S proteasomes, ubiquitin, and protein substrates of proteasome. *Mol. Biol. Cell* **13**, 2771-2782.

Lain, S., Midgley, C., Sparks, A., Lane, E. B. and Lane, D. P. (1999). An inhibitor of nuclear export activates the p53 response and induces the localization of HDM2 and p53 to U1A-positive nuclear bodies associated with the PODs. *Exp. Cell Res.* **248**, 457-472.

Lallemand-Breitenbach, V., Zhu, J., Puvion, F., Koken, M., Honore, N., Doubeikovsky, A., Duprez, E., Pandolfi, P. P., Puvion, E., Freemont, P. et al. (2001). Role of promyelocytic leukemia (PML) sumolation in nuclear body formation, 11S proteasome recruitment, and As(2)O(3)-induced PML or PML/retinoic acid receptor alpha degradation. *J. Exp. Med.* **193**, 1361-1372.

LaMorte, V. J., Dyck, J. A., Ochs, R. L. and Evans, R. M. (1998). Localization of nascent RNA and CREB binding protein with the PML-containing nuclear body. *Proc. Natl. Acad. Sci. USA* **95**, 4991-4996.

Luciani, J. J., Depetris, D., Usson, Y., Metzler-Guillemain, C., Mignon-Ravix, C., Mitchell, M. J., Megarbane, A., Sarda, P., Sirma, H., Moncla, A. et al. (2006). PML nuclear bodies are highly organised DNA-protein structures with a function in heterochromatin remodelling at the G2 phase. *J. Cell Sci.* **119**, 2518-2531.

Mattsson, K., Pokrovskaja, K., Kiss, C., Klein, G. and Szekely, L. (2001). Proteins associated with the promyelocytic leukemia gene product (PML)-containing nuclear body move to the nucleolus upon inhibition of proteasome-dependent protein degradation. *Proc. Natl. Acad. Sci. USA* **98**, 1012-1017.

Maul, G. G., Negorev, D., Bell, P. and Ishov, A. M. (2000). Review: properties and assembly mechanisms of ND10, PML bodies, or PODs. *J. Struct. Biol.* **129**, 278-287.

Meroni, G. and Diez-Roux, G. (2005). TRIM/RBCC, a novel class of 'single protein RING finger' E3 ubiquitin ligases. *BioEssays* **27**, 1147-1157.

Morency, E., Coute, Y., Thomas, J., Texier, P. and Lomonte, P. (2005). The protein ICP0 of herpes simplex virus type 1 is targeted to nucleoli of infected cells. Brief report. *Arch. Virol.* **150**, 2387-2395.

Nabetani, A., Yokoyama, O. and Ishikawa, F. (2004). Localization of hRad9, hHus1, hRad1, and hRad17 and caffeine-sensitive DNA replication at the alternative lengthening of telomeres-associated promyelocytic leukemia body. *J. Biol. Chem.* **279**, 25849-25857.

Pearson, M., Carbone, R., Sebastiani, C., Cioce, M., Fagioli, M., Saito, S., Higashimoto, Y., Appella, E., Minucci, S., Pandolfi, P. P. et al. (2000). PML regulates p53 acetylation and premature senescence induced by oncogenic Ras. *Nature* **406**, 207-210.

Politz, J. C., Polena, I., Trask, I., Bazett-Jones, D. P. and Pederson, T. (2005). A nonribosomal landscape in the nucleolus revealed by the stem cell protein nucleostemin. *Mol. Biol. Cell* **16**, 3401-3410.

Reymond, A., Meroni, G., Fantozzi, A., Merla, G., Cairo, S., Luzi, L., Riganelli, D., Zanaria, E., Messali, S., Cainarca, S. et al. (2001). The tripartite motif family identifies cell compartments. *EMBO J.* **20**, 2140-2151.

Rokaeus, N., Klein, G., Wiman, K. G., Szekely, L. and Mattsson, K. (2006). PRIMA-1(MET) induces nucleolar accumulation of mutant p53 and PML nuclear body-associated proteins. *Oncogene* **26**, 982-992.

Salomoni, P. and Pandolfi, P. P. (2002). The role of PML in tumor suppression. *Cell* **108**, 165-170.

Scaglioni, P. P., Yung, T., Cai, L. F., Erdjument-Bromage, H., Kaufman, A., Singh, B., Teruya-Feldstein, J., Tempst, P. and Pandolfi, P. P. (2006). A CK2-dependent pathway for PML degradation upon cellular and oncogenic stress. *Cell* **126**, 269-283.

Seker, H., Rubbi, C., Linke, S. P., Bowman, E. D., Garfield, S., Hansen, L., Borden, K. L., Milner, J. and Harris, C. C. (2003). UV-C-induced DNA damage leads to p53-dependent nuclear trafficking of PML. *Oncogene* **22**, 1620-1628.

Shav-Tal, Y., Blechman, J., Darzacq, X., Montagna, C., Dye, B. T., Patton, J. G., Singer, R. H. and Zipori, D. (2005). Dynamic sorting of nuclear components into distinct nucleolar caps during transcriptional inhibition. *Mol. Biol. Cell* **16**, 2395-2413.

Shen, T. H., Lin, H. K., Scaglioni, P. P., Yung, T. M. and Pandolfi, P. P. (2006). The mechanisms of PML-nuclear body formation. *Mol. Cell* **24**, 331-339.

Short, K. M. and Cox, T. C. (2006). Subclassification of the RBCC/TRIM superfamily reveals a novel motif necessary for microtubule binding. *J. Biol. Chem.* **281**, 8970-8980.

Torres, C., Lewis, L. and Cristofalo, V. J. (2006). Proteasome inhibitors shorten replicative life span and induce a senescent-like phenotype of human fibroblasts. *J. Cell. Physiol.* **207**, 845-853.

Urano, T., Saito, T., Tsukui, T., Fujita, M., Hosoi, T., Muramatsu, M., Ouchi, Y. and Inoue, S. (2002). Efp targets 14-3-3 sigma for proteolysis and promotes breast tumour growth. *Nature* **417**, 871-875.

Wang, Z. G., Delva, L., Gaboli, M., Rivi, R., Giorgio, M., Cordon-Cardo, C., Grosveld, F. and Pandolfi, P. P. (1998). Role of PML in cell growth and the retinoic acid pathway. *Science* **279**, 1547-1551.

Wu, G., Lee, W. H. and Chen, P. L. (2000). NBS1 and TRF1 colocalize at promyelocytic leukemia bodies during late S/G2 phases in immortalized telomerase-negative cells. Implication of NBS1 in alternative lengthening of telomeres. *J. Biol. Chem.* **275**, 30618-30622.

Yeager, T. R., Neumann, A. A., Englezou, A., Huschtscha, L. I., Noble, J. R. and Reddel, R. R. (1999). Telomerase-negative immortalized human cells contain a novel type of promyelocytic leukemia (PML) body. *Cancer Res.* **59**, 4175-4179.

Journal of Cell Science

Fig S1A

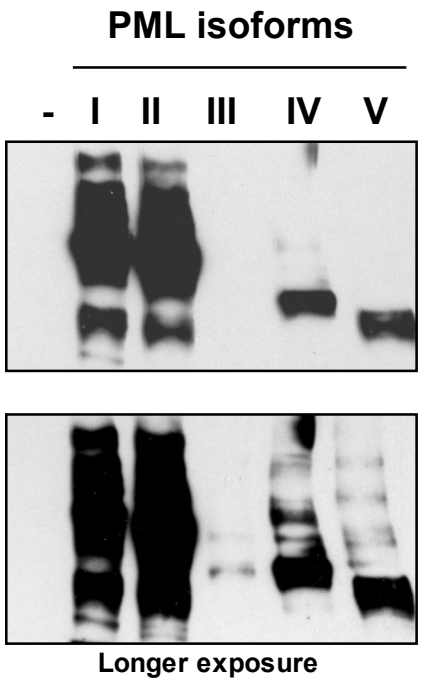

Fig S1B

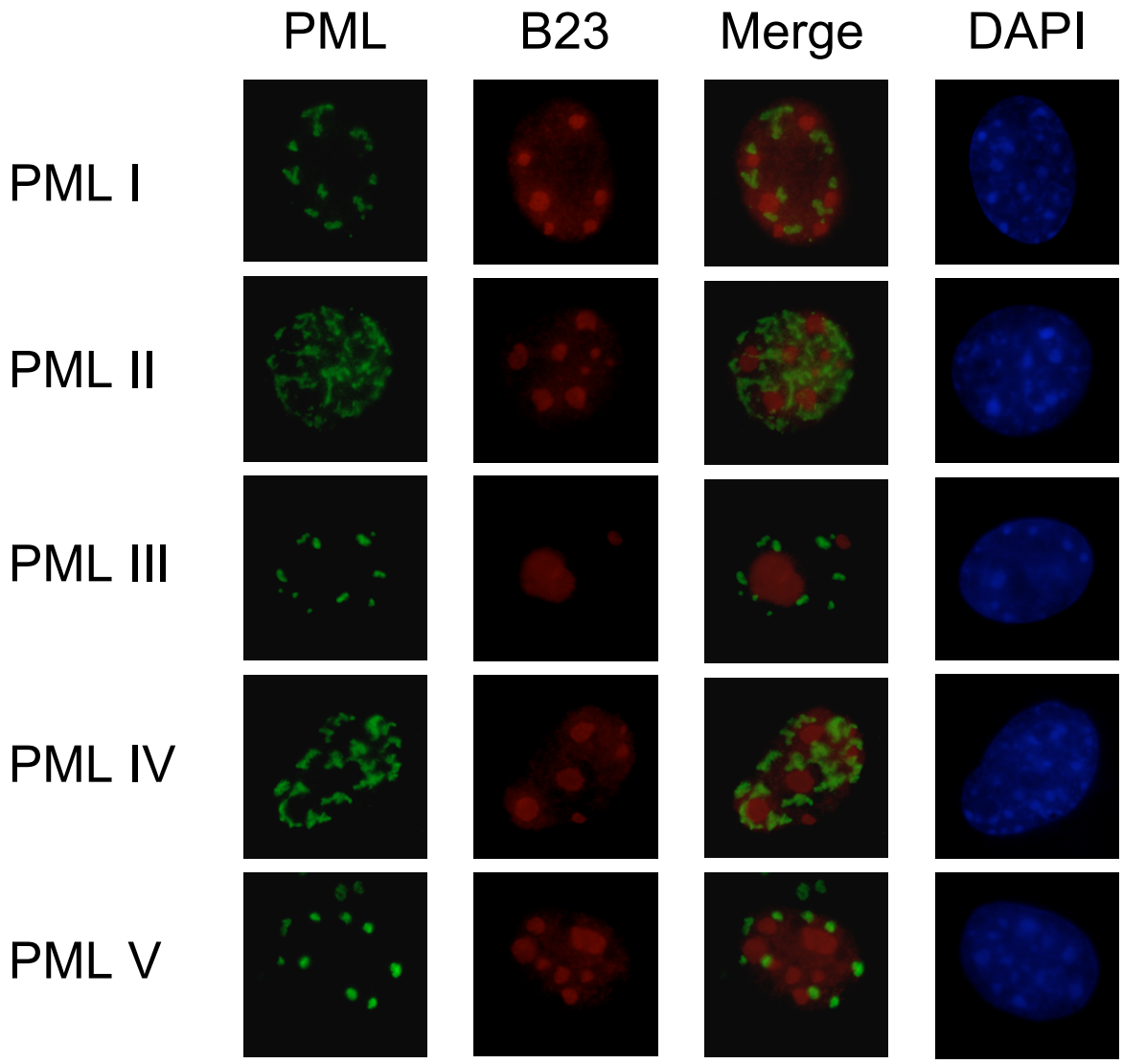

Fig S1C

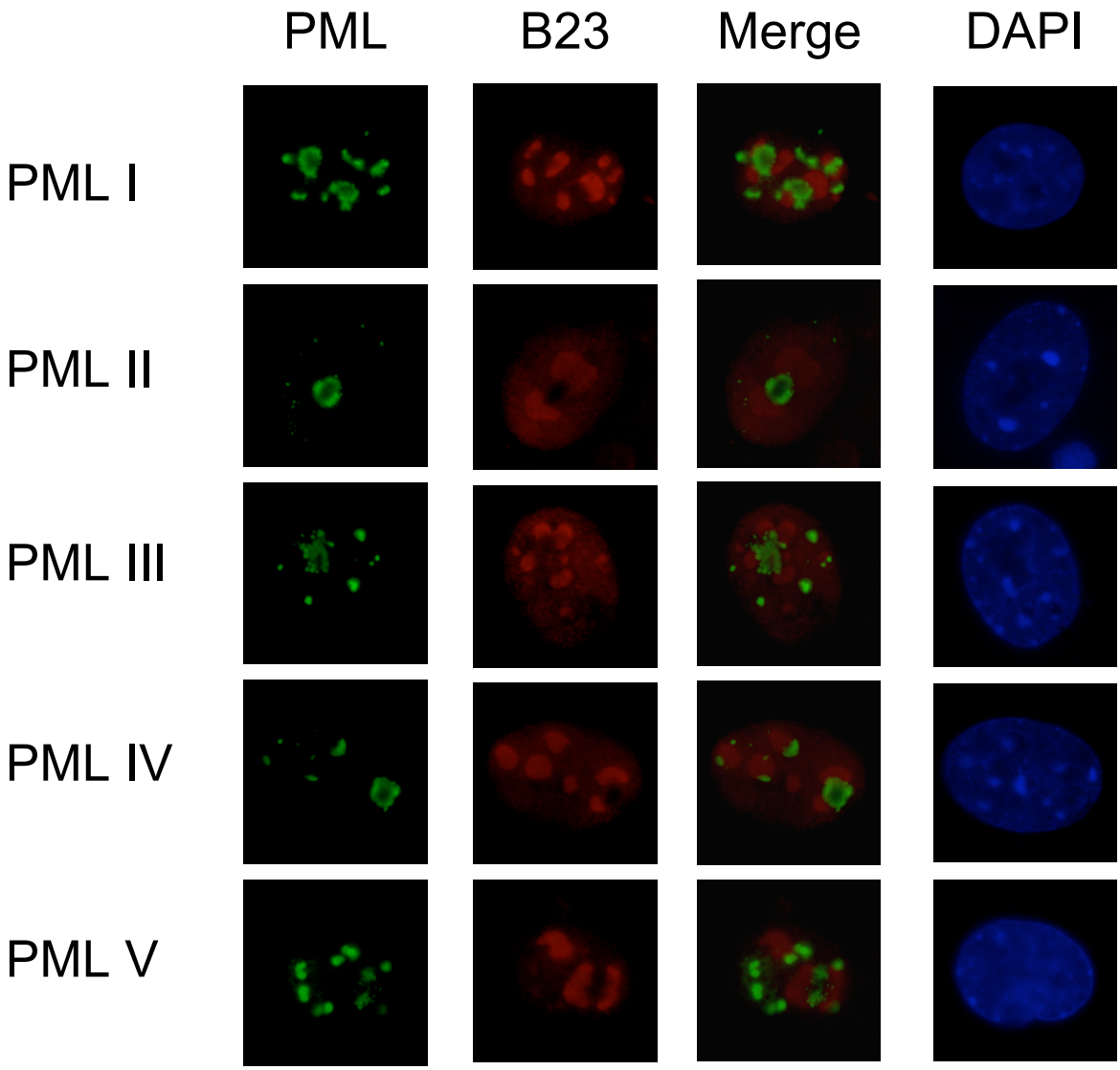

Fig S1D

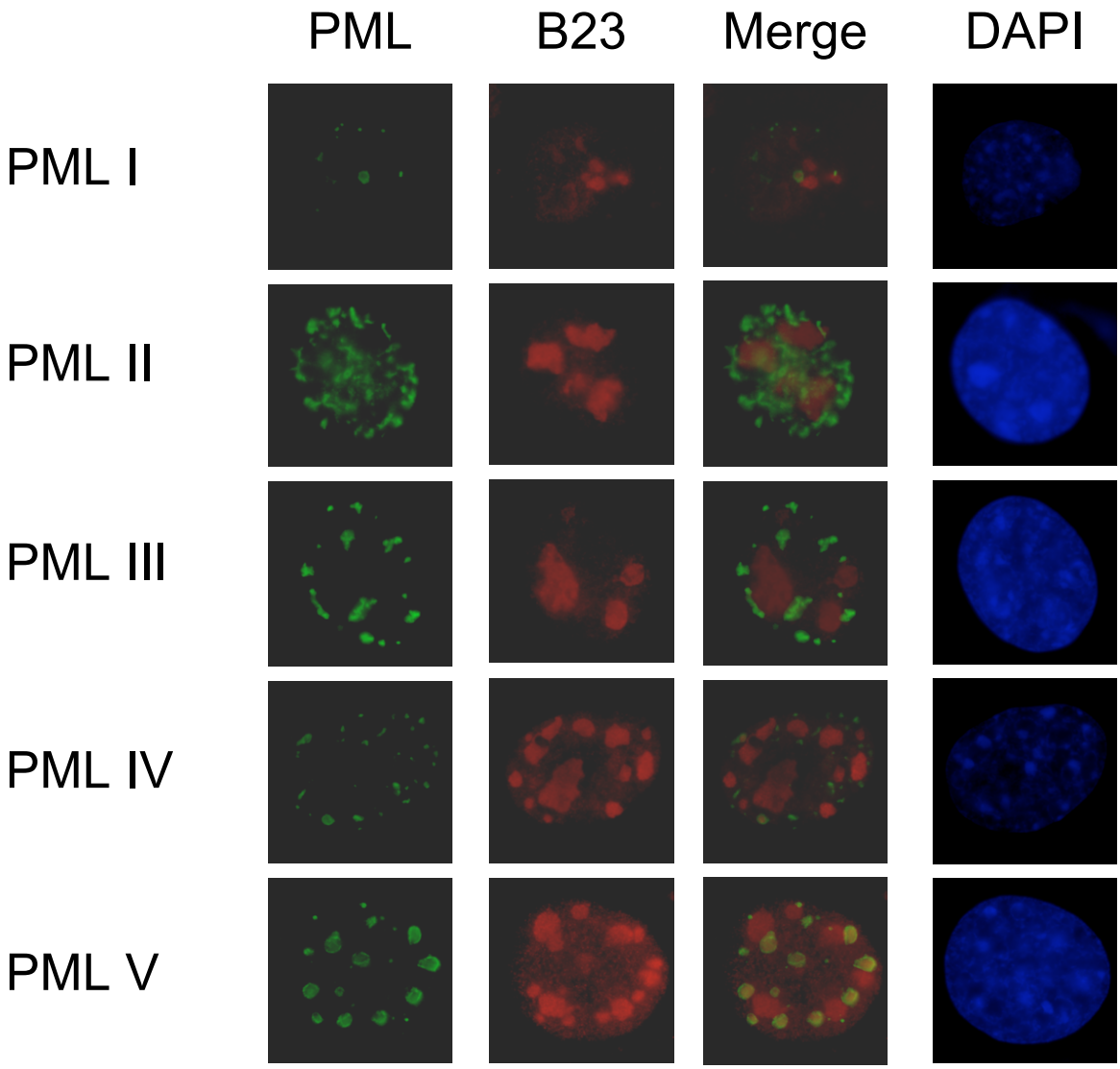

Fig S1E

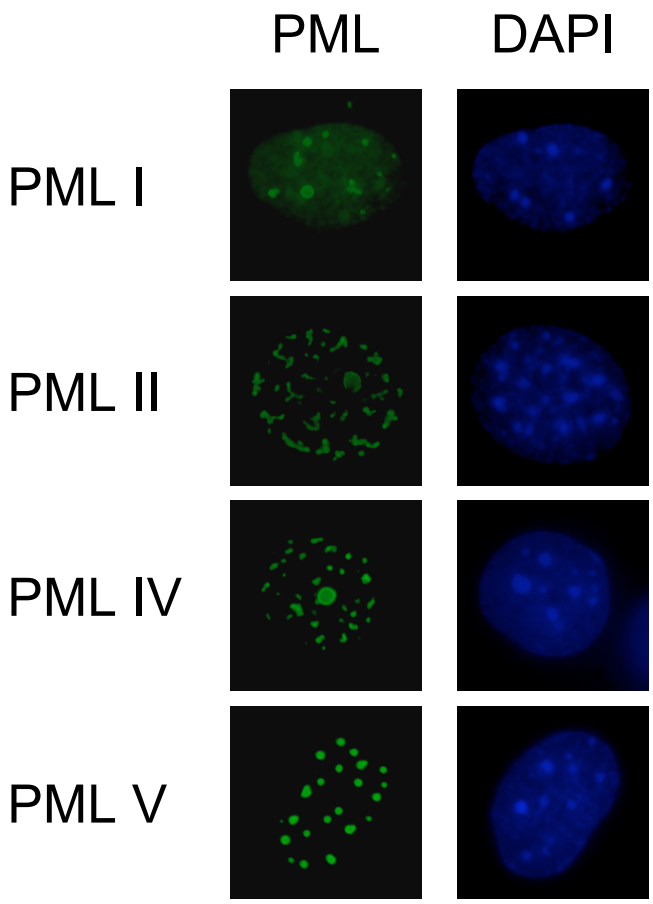

Fig S1F

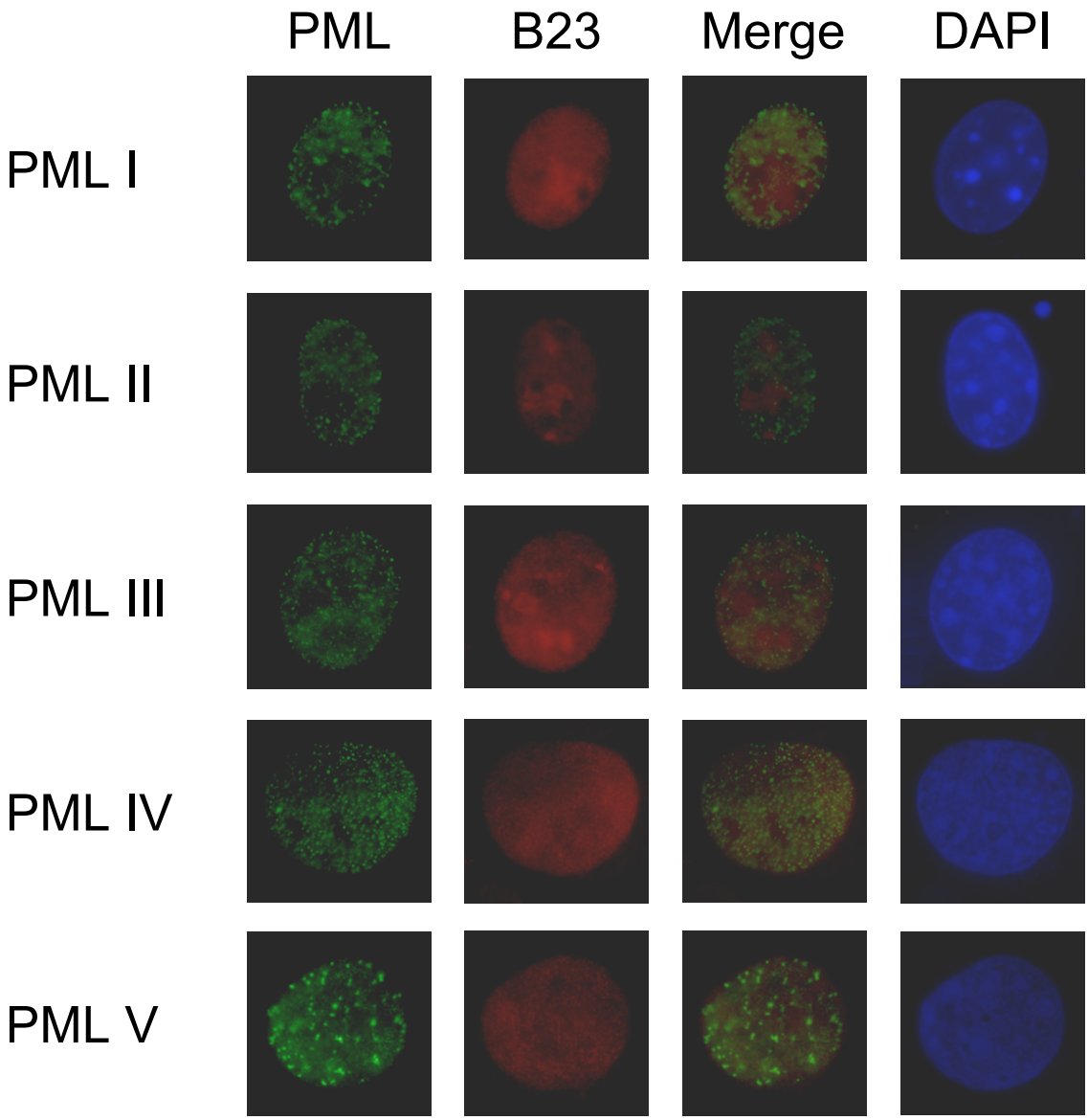

Fig S1G

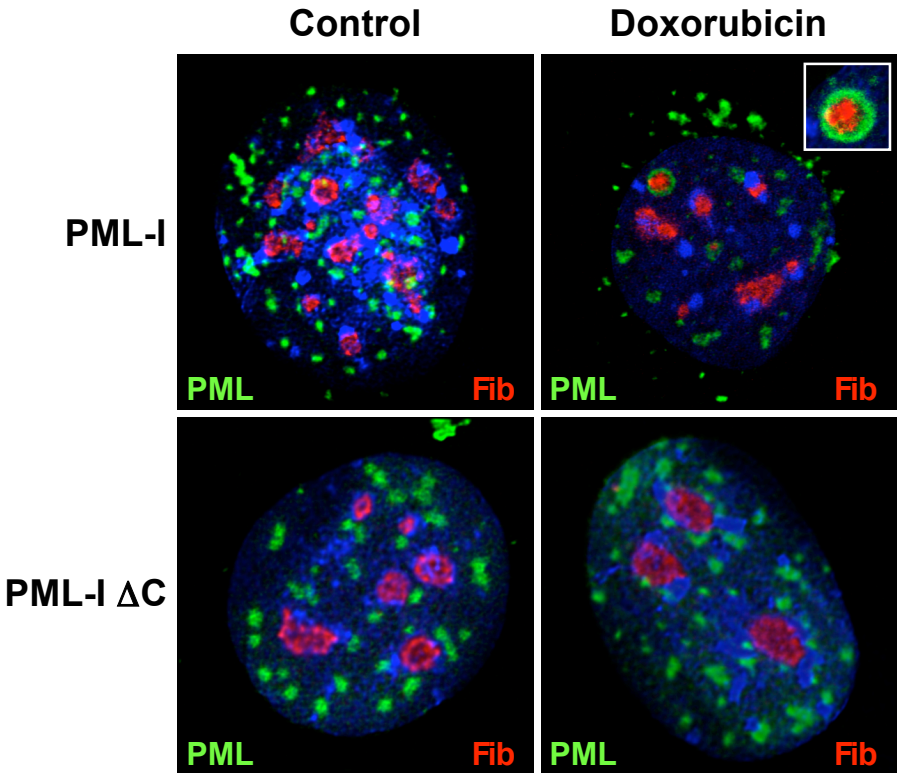
Control
Doxorubicin
PML-I
PML-I ΔC
PML
Fib
PML
Fib
PML
Fib
PML
Fib

Figure S2A


Human SSRELDDSSSESSDLQLEGPSTLRVLDENLADPQAEDRPLVFFDLKIDNETQKISQLAAVNRESKFRVVIQPEAFFSIYSKAVS-LEVGLQHFLSFLSSMRRPILACYKLWGPGLPNFFR
Mouse SSHELDDSSSESSSLQLEGPNSLKALDESLAEPHLEDRTLVFFDLKIDNETQKISQLAAVNRESKFRVLIQPEAFS-VYSKAVS-LEAGLRHFLSFLTTMHRPILACSRLWGPGLPIFFQ
Rat ASHELDDSSSESSSIQLEGPNSLKALDESLAEPHLEDRTLVFFDLKIDNETQKISQLAAVNRESKFRVLIQPEAFS-VYSKAVS-LESGLQHFLSFLNSMHRPLLACPRLWGPGLPIFFQ
Chimp -SRELDDSSSESSDLQLEGPSTLRVLDENLADPQAEDRPLVFFDLKIDNETQKISQLAAVNRESKFRVVIQPEAFFSIYSKAVS-LEVGLQHFLSFLSSMRRPILACYKLWGPGLPNFFR
Cat ----------QLAAVNRESEFRVLIQPEAFFSIYSKAVS-LEVGLQHFLGFLGSMRRPILACYKLWGPGLPNFFR
Dog SSRELDDSSSESSDLQLEGPSSLRVLDNSLADPQAEDRPLVFFDLKIDSESQKISQLAAVNRESEFRVLIQPQAYSSMFSKAVS-LEVGLQHFLGFLGSMRRPVLACSKLWGPSLPIFFR
Bull DSRELADNSSESSDLQLEGPSSLGVLDDSPSNSLVEDKPLVFFDLKIDNETQKISQLAAVNQESQFRALIQPEVLN-VYSKAVS-LEVGLQHFLHFLASMRQPILACYKLWGPSLPSFFQ
Boar SSQEQDNSSSEASDLQLEGPSSLGVLDESLINSGAEDRPLVFFDLKIDSESQKISQLAAVNQESQFRMLIQPEAFT-IRSKAVS-LEVGLQHFLHFLGNMRQPILACYKLWGPGLPSLFR
Elephant ----------QKISQLAAVNRESKFRVLIQPKAFFSIYSKAVS-LEVGLRHFLRFLGSMHRPILACYKLWGPSLPKFFQ
Chicken -DPSLLDDMLEDGTSRDNSHLPICLKN----TLDVGQGSVIFFDVEIWKN--EVIQMSVVDKEKMLSVIIQPMMCLPTSPAITNSYEMGLRDLLSHLSTIRRPILAAFDLWSLPFPTLLK
Human ALEDINRLWEFQEAISGFLAALPLIRERVPGASSFKLKNLAQTYLARNMSE-RSAMAAVLAMRDLCRLLEVSPGPQLAQHVYPFSSLQCFASLQPLVQAAVLPRAEARLLALHNVSFMEL
Mouse TLSDINKLWEFQDTISGFLAVLPLIRERIPGASSFKLGNLAKTYLARNMSE-RSALASVLAMRDLCCLLEISPGLPLAQHIYSFSSLQCFASLQPLIQASVLPQSEARLLALHNVSFVEL
Rat ALNDINKLWEFQDAISGFLAVLPLIQERIPSASSFKLRNLAKTYLARNMSE-RSALAAVLAMRDLCCLLEVSPGLQLAQHIYSFSSLQCFASLQPLIQAQVLPQPEARLLALHNVSFLEL
Chimp ALEDINRLWEFQEAISGFLAALPLIRERVPGASSFKLKNLAQTYLARNMSE-RSAMAAVLAMRDLCRLLEVSPGPQLAQHVYPFSSLQCFASLQPLVQAAVLPRAEARLLALHNVSFMEL
Cat ALEDMNRLWEFQEVISGFLAALPLIRERVPRASSFKLKSLAKTYLARNMSE-RSALAAVLAMRDLCRLLEVSPGPQLAQHVYSFSSLQCFASLQPLVQAAALLRAEARLLALHNVSFTEL
Dog ALEDMNRLWGFQEAISGFLAVLPLVRERVPQASSFRLRSLAKTYLARNVNE-RSALATVLALRDLCRLLEISPGPWLAQHVYSFSSLQCFASLQPLVQAAALAQAQARLLALHNVSFTEL
Bull ALEEMNMLGKFQKSISGFLATLPLIRECVPGASSFKLKSLAKTYLARNMSE-RSALAAVLTMRDLCRLLEVSPSPQLALHVHPFSSLQCFSSLQPLVRAAILPRAEARLLALHKVTFIEL
Boar ALEDMNRLQEFRKAISGFLAILPLIRECVPGASSFKLKNLAETYLARNMNETRSALASVVTMRDLCRLLEVTPGPQLGPHIHSFSCLQCFSSLQPLVRAAVLPRAKARLLALHKVSFLEL
Elephant ALEDMNSLWEFQESISGLLATLPLIREQIPGASSFKLKNLAKTYLARNVNE-RSALASVLAMRDLCRLLEVFP---EARHIYSFSNLQCFASLQPLVRAAVLPLAEARLLALHNVSFEEL
Chicken SLMAIGKKEEFFSMVYGFLDVLPLIKEKIPMKESCKLKNLASNLLWRDLSS-SSTLESARATKDLCNVLEIDLK-SKPRQLLSLANLESFMSLQPLLDKRLLSRPSAQTLASHGIGLPEL
Human LSAHRRDRQGGLKKYSRYLSLQTTT---LPPAQPAFNLQALGTYFEG-LLEGPALARAEGVSTPLAGRGLAERASQQS
Mouse LNAYRTNRQEGLKKYVHYLSLQTTPLSSSASTQVAQFLQALSTHMEG-LLEGHAPAGAEG-------KAESKGCLA--
Rat LTAYRSNRQEGLKKYVHYLSLQTTP--SSASTQIAQFLQALSAYMDG-QLEGHIPAGAEGTALSLSGRAENKGCLA--
Chimp LSAHRRDRQGGLKKYSRYLSLQTTT---LPPAQPAFNLQALGTYFEG-LLEGPALARAEGVSTPLAGHGLAERASQQS
Cat LTAHRRDPERGLKKYSRYLSLQTTS---SPPMQRAVNLQALSSYFKG-LSEEAAVARAEG----IAGHSLAEKAPQQS
Dog LAAHRRDPQQGLKKYSRYLGPQTST---SPPSQRAVSLQALSTYFKG-RSEGAVSAPAQGLSTLLTGHSFAKRACQQS
Bull LTAHHHDPQGGLKKYNRFLSLQSPT---S--SQPVFDLHSLGTYFEG-LLGAPASAGAGGVAAPPAGHSLAERATQQT
Boar VTAHHHDPQEGLKKYNCFLSPQSPS---SPPTQSAFNLQALGTYFDKGLREGLASTKAEGSSSLLTDHSLVERASQES
Elephant LAAHRCDPQGAFKKYSQYLSPQAAP---APPTQPAFDLQVLSAYFAG-LL----------
Chicken HACFACDPIRGLPKMCAVVNAHRHP-----SEKKVRHLSKVKAYFQQQPLAGSSHALVHDELLEAMKTKQDC------

Figure S2B

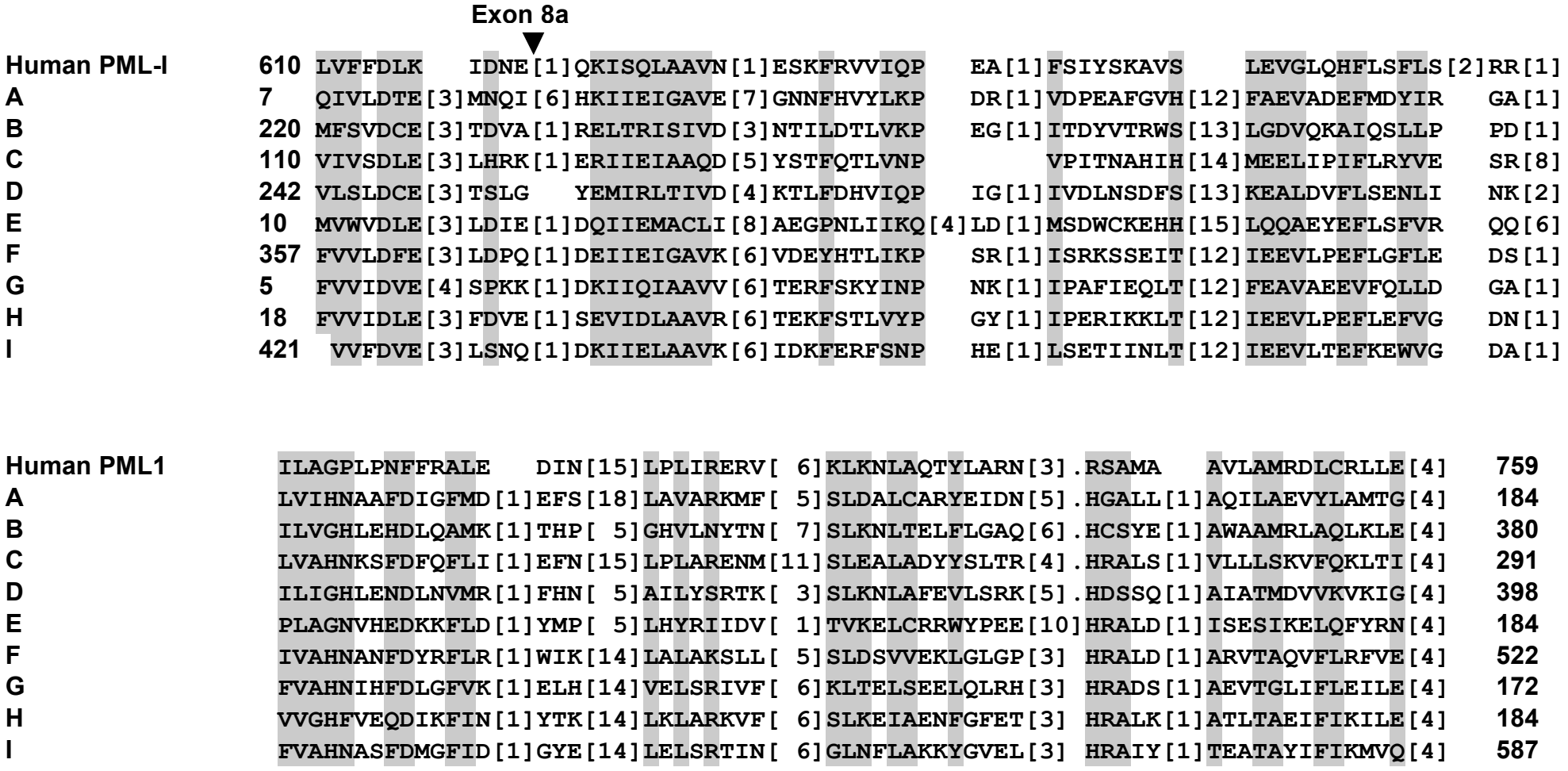
Exon 8a
Human PML-I 610 LVFFDLK IDNE[1]QKISQLAAVN[1]ESKFRVVIQP EA[1]FSIYSKAVS LEVGLQHFLSFLS[2]RR[1]
A 7 QIVLDTE[3]MNQI[6]HKIIEIGAVE[7]GNNFHVYLKP DR[1]VDPEAFGVH[12]FAEVADEFMDYIR GA[1]
B 220 MFSVDCE[3]TDVA[1]RELTRISIVD[3]NTILDTLVKP EG[1]ITDYVTRWS[13]LGDVQKAIQSLLP PD[1]
C 110 VIVSDLE[3]LHRK[1]ERIIEIAAQD[5]YSTFQTLVNP VPITNAHIH[14]MEELIPIFLRYVE SR[8]
D 242 VLSLDCE[3]TSLG YEMIRLTIVD[4]KTLFDHVIQP IG[1]IVDLNSDFS[13]KEALDVFLSENLI NK[2]
E 10 MVWVDLE[3]LDIE[1]DQIIEMACLI[8]AEGPNLIIKQ[4]LD[1]MSDWCKEHH[15]LQQAEYEFLSFVR QQ[6]
F 357 FVVLDFE[3]LDPQ[1]DEIIEIGAVK[6]VDEYHTLIKP SR[1]ISRKSSEIT[12]IEEVLPEFLGFLE DS[1]
G 5 FVVIDVE[4]SPKK[1]DKIIQIAAVV[6]TERFSKYINP NK[1]IPAFIEQLT[12]FEAVAEEVFQLLD GA[1]
H 18 FVVIDLE[3]FDVE[1]SEVIDLAAVR[6]TEKFSTLVYP GY[1]IPERIKKLT[12]IEEVLPEFLEFVG DN[1]
I 421 VVFDVE[3]LSNQ[1]DKIIELAAVK[6]IDKFERFSNP HE[1]LSETIINLT[12]IEEVLTEFKEWVG DA[1]
Human PML1 ILAGPLPNFFRALE DIN[15]LPLIRERV[6]KLKNLAQTYLARN[3].RSAMA AVLAMRDLCRLLE[4] 759
A LVIHNAAFDIGFMD[1]EFS[18]LAVARKMF[5]SLDALCARYEIDN[5].HGALL[1]AQILAEVYLAMTG[4] 184
B ILVGHLEHDLQAMK[1]THP[5]GHVLNYTN[7]SLKNLTELFLGAQ[6].HCSYE[1]AWAAMRLAQLKLE[4] 380
C LVAHNKSFDFQFLI[1]EFN[15]LPLARENM[11]SLEALADYYSLTR[4].HRALS[1]VLLLSKVFQKLTI[4] 291
D ILIGHLENDLNVMR[1]FHN[5]AILYSRTK[3]SLKNLAFEVLSRK[5].HDSSQ[1]AIATMDVVKVKIG[4] 398
E PLAGNVHEDKKFLD[1]YMP[5]LHYRIIDV[1]TVKELCRRWYPEE[10]HRALD[1]ISESIKELQFYRN[4] 184
F IVAHNANFDYRFLR[1]WIK[14]LALAKSLL[5]SLDSVVEKLGLGP[3] HRALD[1]ARVTAQVFLRFVE[4] 522
G FVAHNIHFDLGFVK[1]ELH[14]VELSRIVF[6]KLTELSEELQLRH[3] HRADS[1]AEVTGLIFLEILE[4] 172
H VVGHFVEQDIKFIN[1]YTK[14]LKLARKVF[6]SLKEIAENFGFET[3] HRALK[1]ATLTAEIFIKILE[4] 184
I FVAHNASFDMGFID[1]GYE[14]LELSRTIN[6]GLNFLAKKYGVEL[3] HRAIY[1]TEATAYIFIKMVQ[4] 587

Figure S3

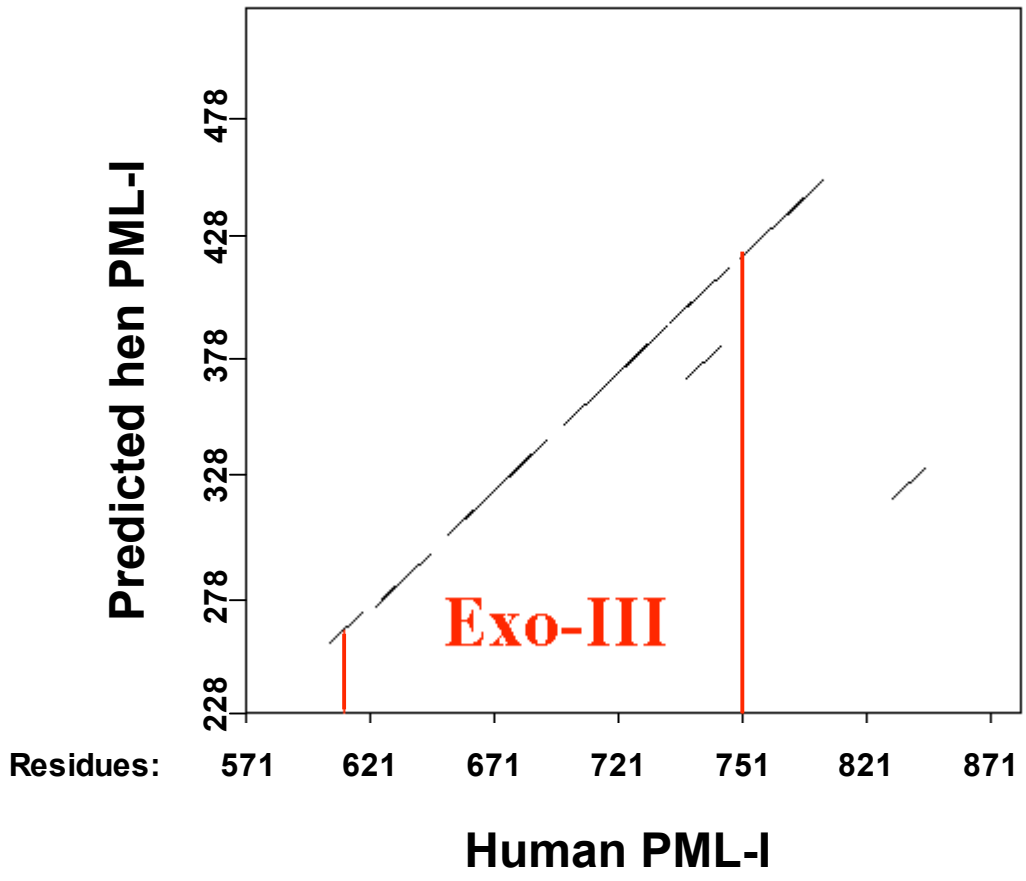
Predicted hen PML-I
478
428
378
328
278
228
Exo-III
Residues:
571
621
671
721
751
821
871
Human PML-I

Figure S4